Journal of Renewable and Sustainable Energy ARTICLE scitation.org/journal/rse

A new MPPT method based on a modified Fibonacci search algorithm for wind energy conversion systems

Cite as: J. Renewable Sustainable Energy **13**, 013304 (2021); doi: 10.1063/5.0035134
Submitted: 27 October 2020 · Accepted: 10 January 2021 ·
Published Online: 17 February 2021

View Online Export Citation CrossMark

İrfan Yazıcı,[1,a] Ersagun Kürşat Yaylacı,[2,b] Barış Cevher,[1,c] Faruk Yalçın,[3,d] and Can Yüzkollar[4,e]

AFFILIATIONS

[1]Department of Electrical and Electronics Engineering, Sakarya University, Sakarya 54050, Turkey
[2]Department of Electrical and Electronics Engineering, Karabuk University, Karabuk 78050, Turkey
[3]Department of Mechatronics Engineering, Sakarya University of Applied Sciences, Sakarya 54050, Turkey
[4]Faculty of Computer and Information Sciences Engineering, Sakarya University, Sakarya 54050, Turkey

[a]iyazici@sakarya.edu.tr
[b]Author to whom correspondence should be addressed: ekyaylaci@karabuk.edu.tr
[c]bcevher@sakarya.edu.tr
[d]farukyalcin@sakarya.edu.tr
[e]can@sakarya.edu.tr

ABSTRACT

In this paper, a new maximum power point tracking (MPPT) method based on the Fibonacci search algorithm (FSA) is proposed for the wind energy conversion system (WECS). The conventional FSA is modified according to the requirements of the WECS to improve its performance as an MPPT algorithm. The performance of the proposed method is investigated for different wind-speed profiles such as step-type and stochastically varied wind speed. Also, the modified FSA based MPPT algorithm is compared with the conventional perturb and observe (CPO) and variable-step PO (VSPO) algorithms. The simulation results approve the superior performance of the proposed method over the CPO and VSPO in terms of maximum power extracted from the system. The real-time performance of the proposed method is also investigated for varying wind conditions in the form of step-up and step-down.

Published under license by AIP Publishing. https://doi.org/10.1063/5.0035134

I. INTRODUCTION

Energy demand is gradually increasing due to population growth and the continuous growth needs of economic systems. As global warming and environmental pollution have been increasing and posing threats to life in recent years, efforts to produce cleaner energy without carbon emissions instead of generating energy from fossil fuels to meet growing energy demand have gradually increased the tendency toward renewable energy sources (RESs). For this reason, renewable energy sources (RESs) are gaining great importance as alternative and accessible energy sources every day. Among renewable energy sources, wind energy occupies an important place because it has the potential to produce 200 times more energy than the energy needed globally.[1]

Wind energy conversion systems (WECSs) have attracted considerable attention in recent years as the fastest-growing distributed energy source due to their zero-carbon emission and cost-effective production among the systems using renewable energy sources. To get an efficient WECS, the WECS must be effectively controlled despite the changing wind speed. Therefore, it is necessary to have sufficient knowledge about the WECSs. The maximum power point tracking (MPPT) algorithm is required for the WECS to operate at its most efficient point. For this purpose, researchers have developed a variety of MPPT methods such as mathematical model-based,[2–8] algorithm-based,[9–20] and hybrid-based.[21–25] A more detailed examination of these studies can be summarized as follows.

In Ref. 2, a comparative analysis of the tip speed ratio (TSR) and the optimal torque (OT) strategies used to utilize maximum wind power in a WECS is presented. In Ref. 3, a voltage-mode second order sliding mode controller (SO-SMC) is proposed to obtain maximum power from the WECS. In Ref. 4, a SO-SMC and a second-order fast terminal SMC are proposed for achieving the maximum wind power and reducing the mechanical stresses. In Ref. 5, an observer-based

finite-time controller is proposed, which is compared with a traditional asymptotic convergent controller. In Ref. 26, the efficiency of the TSR-MPPT method in the WECS was increased by using an integral SMC, which is compared to the conventional SMC. In Ref. 27, a new design of the double integral SMC for switching the boost converter as a mechanical sensorless MPPT method in the WECS is presented, which is compared to the conventional SMC. In Ref. 8, a new decoupled proportional and integral (PI) current controller, developed using the combination of feedback linearization and disturbance observer-based control techniques, is designed to increase the nominal transient performance of the PI controller under model uncertainty. In Ref. 9, an experimental comparative analysis of the MPPT methods such as perturb and observe (PO) and incremental conductance (IC) is presented. In Refs. 10–13, the problems in conventional PO (CPO) algorithms are solved by newly proposed MPPT algorithms such as a performance-improved adaptive PO, a hybrid PO, and a modified PO. In Ref. 14, the comparative analysis of algorithm-based MPPT methods such as PO, IC, and particle swarm optimization (PSO) is performed. In Ref. 15, a neural network tuned controller using a radial basis function-based neural network as a MPPT method has been proposed. In Ref. 16, a new adaptive PO algorithm is proposed as an MPPT control method to capture maximum power from the WECS. In Ref. 17, the comparative analysis of PO and IC algorithms used for MPPT is presented. In Ref. 18, a three-level boost converter topology is chosen instead of the traditional boost converter in the WECS. Comparative analysis of MPPT methods such as the PO algorithm and a fuzzy logic controller (FLC) used as the switching method of a three-level boost converter is presented. In Ref. 19, an optimal FLC-based MPPT inverter is developed to maximize energy efficiency in a grid-connected WECS. In Ref. 20, an artificially intelligent technique based on the FLC is proposed to develop MPPT and is compared with traditional MPPT methods. In Ref. 21, a model predictive control is proposed to overcome the problem of the CPO method. In Ref. 22, a hybrid MPPT strategy based on an improved extreme learning machine with the Bat Algorithm is proposed to estimate the wind speed in a WECS operating parallel to the grid. In Ref. 23, comparative analysis and simulation of three MPPT control methods such as a PI controller, a Fuzzy-PI, and an adaptive FLC-PI controller are shown. In Ref. 24, adaptive Type-1 and Type-2 fuzzy logic fractional proportional and integral (PI) controllers are designed for the permanent magnet synchronous generator (PMSG)-based WECS. In Ref. 25, a new fast terminal SMC based MPPT controller and a new hybrid MPPT method combining chaotic-based PSO derivatives with an optimal relation-based method are proposed. In Ref. 28, an artificial neural network and a particle swarm optimization based observer were developed for wind speed prediction. Also, a direct adaptive fuzzy-PI controller was used as a TSR based MPPT controller.

Among the MPPT methods, main methods such as mathematical model-based tip speed ratio (TSR), power signal feedback (PSF), and optimal torque (OT) have a fast response because they have the speed knowledge.[29] Despite this advantage, they suffer from more complex structures and increased system costs due to the need for additional measurements. On the other hand, algorithm-based methods such as perturb and observe (PO), hill climb search (HCS), and incremental conductance (IC) are the most prominent MPPT methods in the literature. The main advantages of these methods are that they require few measurements and have a relatively simple structure. Power oscillation around the MPP due to trial and error process is one of the main problems of these methods. Besides, the selection of the optimal step size in terms of the speed of reaching the MPP point and system efficiency is another important task that must be overcome in the use of these algorithms. Many researchers contributed to the development of WECSs by presenting valuable studies to the literature to overcome these problems.

The Fibonacci search algorithm (FSA) is a one-dimensional search algorithm with high computational efficiency since it uses variable step size and symmetrical step length.[30,31] In Ref. 32, Miyatake *et al.* proposed a FSA based MPPT method for the photovoltaic (PV) systems, which features simplicity in computations and fast convergence. Miyatake *et al.* modified and developed the FSA based MPPT for partially shaded photovoltaic systems by changing the search range with a new function in Refs. 33 and 34. In Ref. 35, Ramaprabha *et al.* modified the FSA by shifting the search range to find the global MPP for the partial shade solar PV array. In Ref. 36, an MPPT method for solar PV systems using fuzzy controls with a modified FSA is offered. In Ref. 37, a modified FSA is developed considering different environmental irradiation effects for PV systems. MPPT methods based on the FSA, which have advantages such as structural simplicity and fast convergence, have been examined in various studies for PV systems, and their performance superiority has been shown. In Ref. 38, a modified FSA is successfully tested on a PV system during non-uniform and rapidly changing irradiation conditions.

The satisfactory performance of the MPPT methods based on the FSA in PV systems and the fact that this method has not yet been examined in the WECS has motivated this study. Since there is no available study in the literature investigating the FSA performance in the WECS, the authors have seen it valuable to analyze the FSA as a new MPPT method for the WECS.

The main contribution of this study can be summarized as follows:

(1) A new MPPT method based on the modified Fibonacci search algorithm (FSA-MPPT) is developed.
(2) The general drawbacks of the algorithm-based MPPT methods such as incorrect control laws for rapidly changing wind speed, choice of step size, and oscillation around the maximum power are being eliminated.
(3) To improve the performance of the proposed MPPT algorithm, the traditional FSA is modified with the ability to detect the wind variation and dynamic search range depending on wind speed.
(4) The performance of the offered method is investigated with the step-type and realistic wind speed profiles. Also, the proposed method is compared under the same conditions as conventional PO (CPO) and variable step PO (VSPO) widely used in the literature.
(5) The real-time performance of the offered method is also investigated. The experiments carried out for varying wind conditions in the form of step-up and step-down have confirmed the superiority of the proposed algorithm.

II. WECS CONFIGURATION

The WECS used in this paper as given in Fig. 1 consists of a wind turbine, a generator, a power converter, and load. It may have different topologies according to the generator and power converter unit used.

Published under license by AIP Publishing

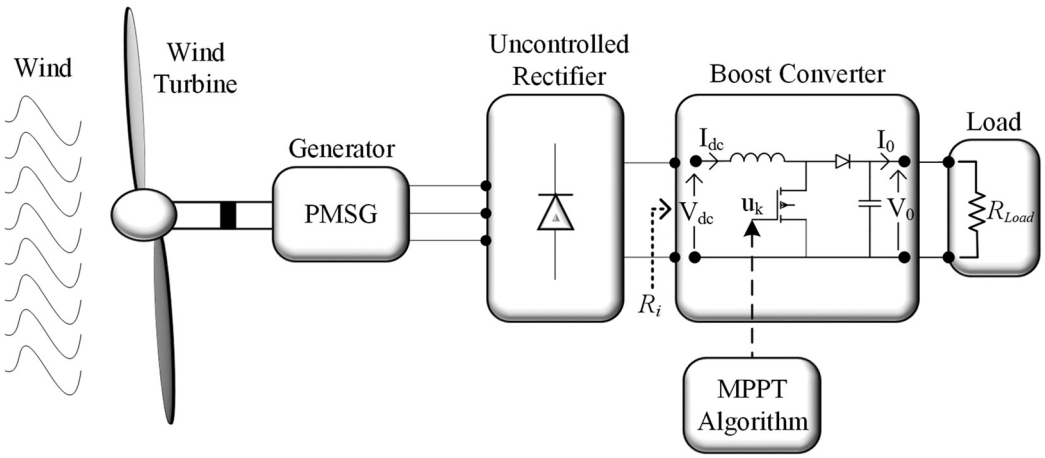

FIG. 1. WECS topology for this paper.

A. Wind Turbine

The mechanical power generated by the wind turbine (P_m) can be given as

$$P_m = 0.5\rho A c_p(\lambda, \beta) {V_w}^3, \tag{1}$$

where V_w is the wind speed, ρ is the air density, A is the swept area by the blades, c_p is the performance coefficient of the turbine, λ is the tip speed ratio, and β is the blade angle (0 for the MPPT region). The c_p equation used in this paper is given as follows:[39]

$$\begin{aligned} c_p(\lambda, \beta) &= c_1\left(\frac{c_2}{\lambda_i} - c_3\beta - c_4\right)e^{-c_5/\lambda_i} + c_6\lambda, \\ \lambda_i &= \frac{1}{\lambda + 0.08\beta} - \frac{0.035}{\beta^3 + 1}, \end{aligned} \tag{2}$$

where in this study coefficients are used as $c_1 = 0.5176$, $c_2 = 116$, $c_3 = 0.4$, $c_4 = 5$, $c_5 = 21$, and $c_6 = 0.0068$ and $\beta = 0$.[39]

c_p will be at its maximum value when the maximum power is extracted from the turbine. Therefore, c_p can be used as an indicator of the performance of the MPPT algorithm. c_{pmax} is only possible when the tip speed ratio (λ) is kept at its optimal value. λ can be expressed as follows:

$$\lambda = \frac{R\omega_m}{V_w}, \tag{3}$$

where R and ω_m are the radius and angular speed of the wind turbine, respectively. The optimal value of λ (λ_{opt}) is calculated as $\lambda_{opt} = 8.1$ by differentiating (2) with respect to λ.[39] It can be concluded from (4) that the MPPT can be assured only by changing the rotational speed for a constant wind speed as follows:

$$\omega_{m-opt} = \lambda_{opt} V_w / R. \tag{4}$$

Also, it can be said from (2) and (4) that ω_{opt} will be changed according to the variation in wind speed.

B. Generator, power converter, and load

The permanent magnet synchronous generator (PMSG) is one of the most used generator types in small-sized and medium-sized WECSs although the various types of generators are used in the WECS.[40,41] The dynamic voltage equations of the PMSG in the d-q reference frames can be written as[42]

$$V_d = -R_s i_d - L_d \frac{di_d}{dt} + \omega_e L_q i_q, \tag{5}$$

$$V_q = -R_s i_q - L_q \frac{di_q}{dt} + \omega_e L_d i_d + \omega_e \lambda_m, \tag{6}$$

where V_d, V_q, I_d, i_q, L_d, and L_q are two-axis machine voltages, currents, and inductances, R_s is the machine resistance per phase, λ_m is the amplitude of the flux linkages provided by the permanent magnet, and $\omega_e = p\omega_m$ is the electrical angular velocity, where p is pole pairs. The electromagnetic torque of the PMSG excited by the wind turbine can be written as follows:

$$T_L = 1.5p\left[(L_d - L_q) i_q i_d - \lambda_m i_q\right]. \tag{7}$$

The output voltage of the PMSG is rectified by an uncontrolled-rectifier. The boost converter is used at the output of the rectifier because of some advantages such as lower cost, higher reliability, and easier control capability.[43,44] The output of the boost converter is connected to a constant resistive load because this paper is mainly focused on an MPPT study.

To get maximum power from the wind, the output load can be changed by modulating the duty ratio (D) of the switching device of the boost converter. The MPPT methods rely on matching the load. For this purpose, the input resistance should be changed because of the constant load resistance. The apparent input resistance of the boost converter (R_i) can be given as follows:[45]

$$R_i \approx (1 - D)^2 R_{load}, \tag{8}$$

where D and R_{load} are the duty ratio and load resistance, respectively. In light of this knowledge, it can be said easily that the rotational speed of the turbine can be set via the D. When D is increased, R_i will reduce, and thereby, the generator current will increase.[46] Eventually, the braking electromagnetic torque (T_L) induced by the generator will increase. Including J, F, and T_m, which are the overall inertia of the system, viscous friction, and turbine torque, the dynamic equation of the wind turbine can be expressed as follows:

Published under license by AIP Publishing

$$T_m - T_L - F\omega_m = J\frac{d\omega_m}{dt}. \quad (9)$$

It is concluded from (9) that the increment in T_L causes a reduction in the angular speed of the wind turbine. It can be said by repeating the same analysis that the reduction of D will cause an increment in the angular speed of the wind turbine.

The WECS parameters are given in Table I for this paper. PMSG parameters used in simulation studies are taken from Ref. 47. Wind turbine and boost converter parameters are determined by taking into consideration the PMSG parameters such as power, voltage, torque, and speed.

In the steady-state state, the relationship between the output voltage (V_0), the input voltage (V_{dc}), and the output current (I_L), the input current (I_{dc}) of the boost-converter can be expressed as follows:[48]

$$V_0 = \frac{V_{dc}}{(1-D)}, \qquad I_0 = I_{dc}(1-D). \quad (10)$$

In general, there are three main parameters to be determined by the designer in the boost converter (BC) design, switching frequency (f_s), inductance (L), and capacitance (C). For BC to operate in continuous-current-mode, L should be selected such that $L > L_k$, where the L_k value is calculated as follows:[48]

$$L_k = \frac{DR_{Load}(1-D)^2}{2f_s}. \quad (11)$$

Similarly, C is determined as follows:

$$C = \frac{D}{R_{Load}\Delta V_0 f_s}, \quad (12)$$

where ΔV_0 is the band of the output voltage ripple. More detailed information for BC is given in Ref. 48.

III. STUDIES ON USED MPPT ALGORITHMS

The proposed FSA based MPPT method for the WECS has been compared with the CPO and VSPO based MPPT algorithms, which are widely used in the literature. The methods used are briefly introduced below.

TABLE I. The WECS parameters used in this paper.

	Description	Parameter	Nominal value
Boost converter	Capacitance	C	1500 μF
	Inductance	L	4.4 mH
	Inductor resistance	r_L	0.15 Ω
	Load resistance	R_{Load}	150 Ω
	Switching frequency	f_s	5 kHz
PMSG	Inertia	J	0.013 kg m^2
	Friction factor	F	0.0425 N m s
	Armature inductance	L_a	0.000 835 H
	Stator resistance	R_s	5 Ω
	Pole pairs	P	8
Wind turbine	Nominal power	P_m	2.2 kW
	Nominal wind speed	$V_{w\text{-}nom}$	12 m/s
	Base rotational speed	$\omega_{m\text{-}base}$	462/322

A. CPO and VSPO algorithm based MPPT methods

In this study, the CPO and VSPO are used to compare the performance of the proposed MPPT algorithm. Since there are many studies[49,50] in the literature examining PO and VSPO based algorithms, it will be briefly mentioned here. In generally, CPO based MPPT algorithms require neither generator nor turbine parameters for the realization. Basically, the CPO based MPPT algorithm depends on introducing a small perturbation to the control variable and observing the extracted power variation until the power slope is zero. However, choosing the optimum step size in CPO in terms of time to reach the MPP and oscillations around MPP is a challenging task. Small step size has disadvantages such as slower convergence to MPP and high transient power losses. The larger step size provides a faster convergence but suffers from oscillations around the MPP, which reduces the overall system efficiency. VSPO algorithms that can be classified as the modified and adaptive PO algorithms offer solutions to the specified problems of CPO.[49,50]

In Fig. 2, the turbine power characteristics for different wind speed are presented. Assume that the system is operated at 1. When the wind speed changed from 8.4 m/s to 12 m/s, the WECS will go to 2. The mechanical power and rotational speed of the wind turbine will increase. To get maximum power, the duty ratio should increase at each sample time until the MPP. Therefore, the system will go to 3. After that, the wind speed decreases 9.6. It means that the system is now at 4. The mechanical power and rotational speed of the wind turbine will also decrease at this point. The duty ratio should decrease to bring the system from 4 to 5. The main working cycle of the CPO and VSPO can be summarized as that for this paper.

The flow chart of the VSPO used in simulation studies is given in Fig. 3. Unlike the CPO, the VSPO method uses three different duty ratios D_1, D_2, and D_3 to get faster MPPT. To avoid oscillations around the MPP and achieve better efficiency, the system will be operated at its optimum value where the maximum power is attained in both methods when MPPT is satisfied. If a sudden change in the power value larger than a specified P_{min} is detected, which means wind speed changed, the algorithm will start the same procedure to track a new MPP.

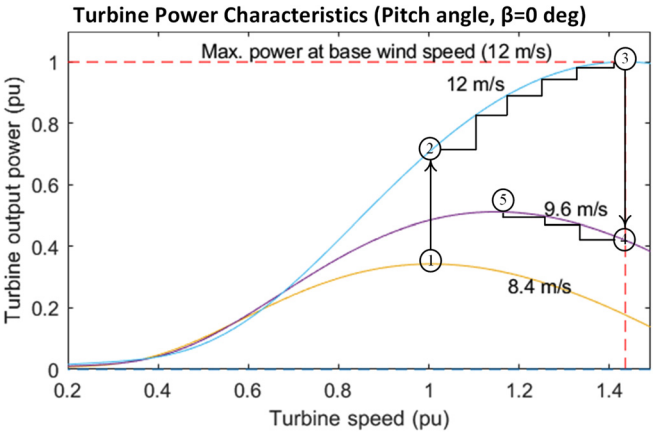

FIG. 2. Turbine power characteristics for different wind speeds.

Published under license by AIP Publishing

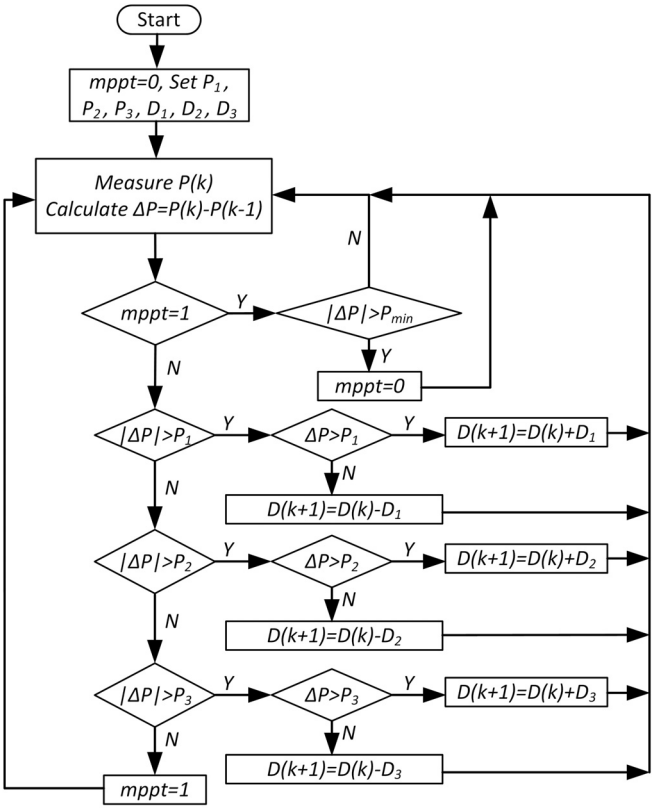

FIG. 3. The flow chart of the VSPO.

B. Fibonacci search algorithm based MPPT method

The FSA is an algorithm relying on the strategy of shifting and restricting the search interval to find the minimum or maximum value of a unimodal function. The shifting direction of the algorithm is specified by evaluating the function at two experiment points. The experimental points are calculated based on the numbers from the

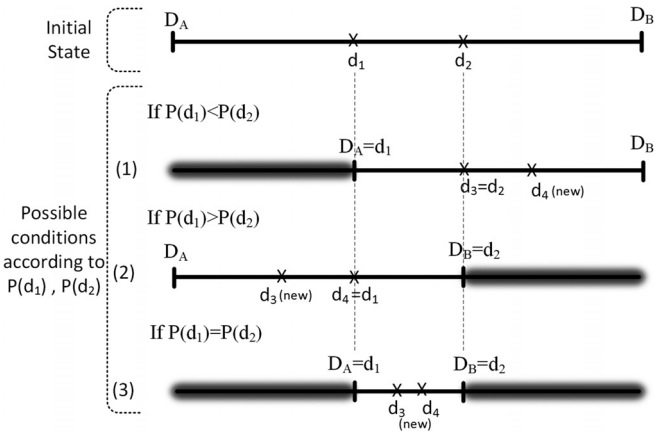

FIG. 4. The FSA search process for maximum.

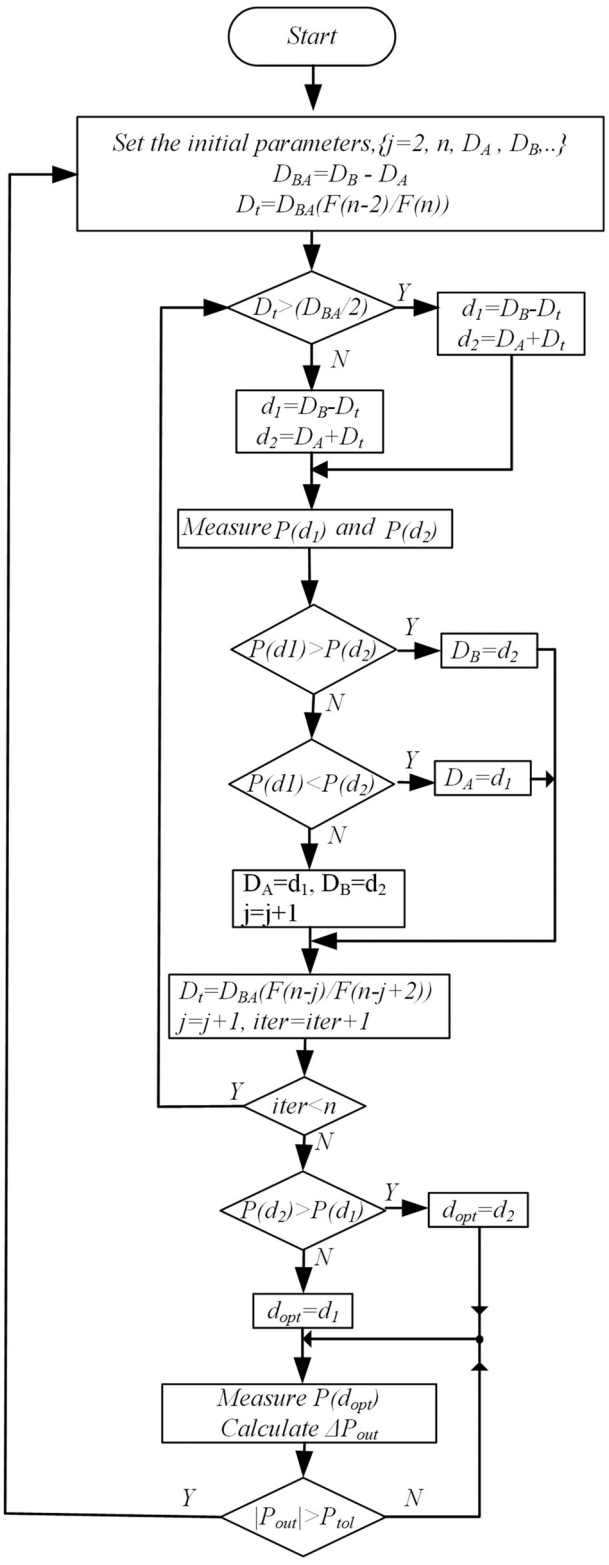

FIG. 5. The flow chart of the proposed FSA.

Published under license by AIP Publishing

Fibonacci sequence. The Fibonacci sequence used in the search algorithm can be defined as follows:[51]

$$F = [F_0, F_1, F_2, \ldots, F_{n-2}, F_{n-1}, F_n], \tag{13}$$

where F_i, $i = 0, 1, \ldots, n$ are the Fibonacci numbers and n is the maximum experiment number tested in the algorithm. The Fibonacci numbers are generated as follows:

$$\begin{aligned} F_0 &= F_1 = 1, \\ F_k &= F_{k-1} + F_{k-2}, \quad k = 2, 3, \ldots, n, \end{aligned} \tag{14}$$

where F_k is the kth Fibonacci number.

Considering the WECS given in Fig. 1, a schematic is given in Fig. 4 to explain the search process of the Fibonacci algorithm easily, where D_A and D_B are the lower and upper limits of the duty cycle and d_1, d_2, d_3, and d_4 are the experiment points where the power value captured from the system is measured.

The initial experiment points of the output powers, d_1 and d_2, are calculated as follows:

$$d_1 = D_A + \left(\frac{F_{n-2}}{F_n}\right)(D_B - D_A), \quad d_2 = D_B - \left(\frac{F_{n-2}}{F_n}\right)(D_B - D_A), \tag{15}$$

where F_n and F_{n-2} are given in (13). After the search interval (D_A or/and D_B) is updated according to the relationship between $P(d_1)$ and $P(d_2)$, the subsequent experiment points for output power are calculated as follows:

$$\begin{aligned} d_3 &= D_A + \left(\frac{F_{n-j}}{F_{n-j+2}}\right)(D_B - D_A), \\ d_4 &= D_B - \left(\frac{F_{n-j}}{F_{n-j+2}}\right)(D_B - D_A), \end{aligned} \tag{16}$$

where j represents a variable with an initial value of $j = 2$ in the FSA.

As shown in Figs. 4 and 5, in the case of $P(d_1) \neq P(d_2)$, only one of d_3 or d_4 will be calculated as a new experiment point, while the other will always be equal to the previous d_1 or d_2 depending on the narrowing direction. In the case of $P(d_1) = P(d_2)$, both d_3 and d_4 are formed

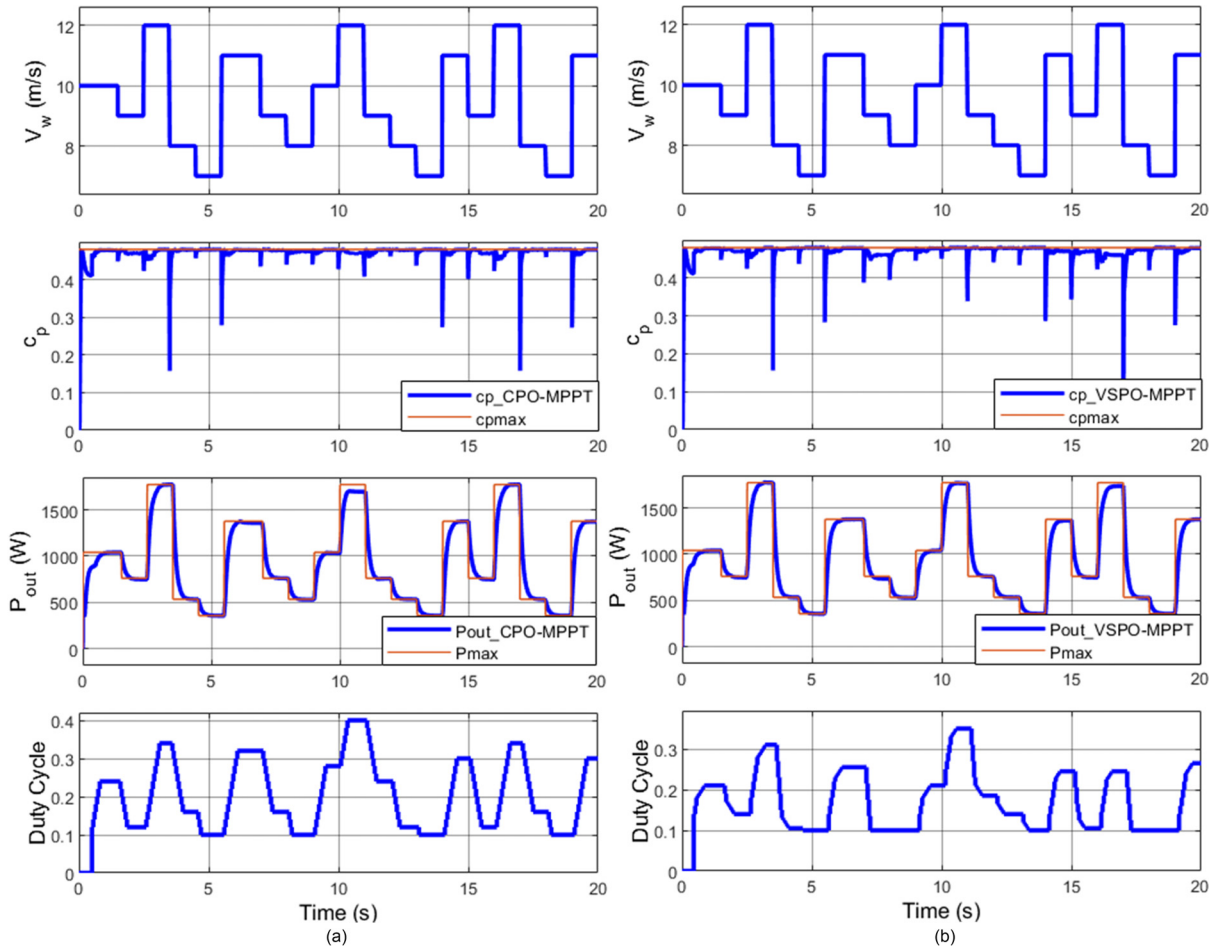

FIG. 6. Performances of the (a) CPO based MPPT and (b) VSPO based MPPT.

Published under license by AIP Publishing

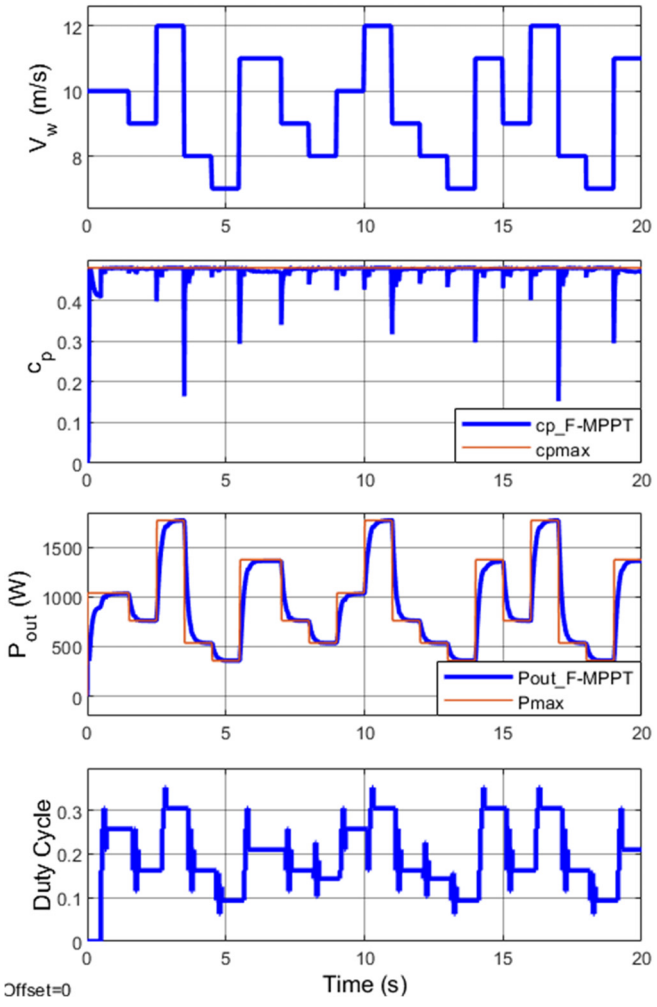

FIG. 7. Performances of the FSA based MPPT.

as new experiment points. The total number of experiments should be determined from (17) before running the algorithm,

$$\frac{L_n}{L_0} = \frac{1}{F_n}, \tag{17}$$

where L_0 is the initial uncertainty interval, L_n is the uncertainty interval after n experiments, and F_n is the last number in the Fibonacci sequence in (13).

The flow chart of the FSA based MPPT method is given in Fig. 5 in detail.

IV. SIMULATION AND EXPERIMENTAL RESULTS AND DISCUSSION

In simulation studies for a fair comparison between the methods, for each one,

(1) The oscillations around the MPPT have been prevented.
(2) The same sample time has been used. The sampling time to run the algorithms can be determined by considering the general time constant value obtained from the step-response of the open-loop system. In simulation studies, the sampling time for all 3 algorithms is taken as $T = 50$ ms.
(3) For detecting the wind speed changing, the same threshold value for output power has been used.

Also, all methods are optimized in terms of the iteration number or step size of the duty cycle. The simulation studies have been realized for two different wind profiles as follows.

A. Scenario 1

As a first scenario, the wind speed is changed as a step-type function in the range 7–12 m/s. The simulation studies have been realized for the same wind speed profile for all investigated methods. During the 20-s simulation period, many different wind speed changes are used as possible. The performance coefficient, output power, and duty cycle are given to compare the performance of the methods. The c_p for the CPO given in Fig. 6(a) deviates from its maximum value for three times at 1.5th, 10th, and 15th seconds. However, the output power given in Fig. 6(a) deviates from its reference value only one time at the 10th second. There is not a conflict in this situation for the WECS because it is known that there are situations where the maximum value of mechanical power may not cross with the maximum electrical output power.[45]

The c_p for the VSPO given in Fig. 6(b) deviates from its maximum value for five times at 1.5th, 7th, 14th, 15th, and 16th seconds. However, the output power given in Fig. 6(b) deviates only one time from its reference value at the 16th second but less than CPO.

For the same wind profile, the performances of the FSA based MPPT method are given in Fig. 7. According to the changing wind speed, the cp value deviates two times in the 6th and 19th seconds. The output power almost does not deviate from the reference value. The variation of the duty cycle is different from the one that occurs in CPO and VSPO due to the natural structure of the FSA.

For clarity, the c_p and P_{out} values are averaged during the simulation period for all methods investigated, and the results are presented in Table II. The proposed method has the best performance in terms of c_p and P_{out}. Another important point is that the average value of

TABLE II. The comparison between the methods for Scenario 1.

Performance criteria	CPO	VSPO	Proposed FSA	Available maximum values
Average of c_p	0.4751	0.4722	0.4756	0.48
Average of P_{out} (W)	933.3	933.7	935.5	947.2
Efficiency %	98.53	98.57	98.76	

Published under license by AIP Publishing

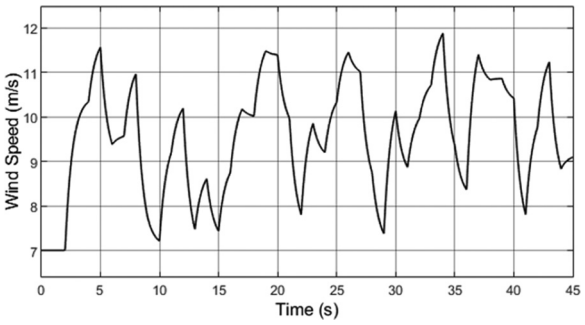

FIG. 8. The applied wind speed for Scenario 2.

P_{out} for VSPO is greater than what CPO provides although the average value of c_p for CPO is larger than that for VSPO. It is pointed out before that the maximum value of the mechanical power cannot be the same as the maximum value of output power.

B. Scenario 2

Although the wind speed is changed as a step function in Scenario 1, the real-time wind speed may have a more complex profile as given in Fig. 8. The performance of the investigated MPPT algorithms in the case of the stochastic wind profile given in Fig. 8 is given in Fig. 9 in terms of c_p and P_{out}. In the case of Scenario 2, the differences between the performances of the investigated methods are seen more clearly. Although the superior performance of the proposed method over the CPO and VSPO can be seen clearly from Fig. 9, the average values of c_p and P_{out} are also given in Table III to make a concrete comparison. In terms of the average power extracted from the system in a 45 s run time, the recommended method reached a value of 21.1 W greater than VSPO and 109 W greater than CPO. Considering the efficiency value, the proposed method can provide 11.41% and 2.2% more energy than CPO and VSPO, respectively.

While the three methods have similar performance in step-type wind changes, the superior performance of the proposed method in the randomly changing wind profile is clearly seen from the efficiency values given in Tables II and III.

C. Experimental studies

The real-time performance of the offered method is also investigated experimentally for various wind conditions using the test-setup given in Fig. 10. For detailed information about the test bench, it can be examined in Refs. 52 and 53. As explained above, although the instantaneous value of c_p varies depending on the wind speed and load value, it reaches a maximum value ($c_{p\text{-}max}$) when the system operates at the optimum point. In the first experiment, as given in Fig. 11, wind with a constant speed of $V = 9$ m/s is applied at $t = t_0$ to show the variation of c_p without the MPPT algorithm and the FSA is not operated until $t = t_{on}$. As seen from Fig. 11, the c_p value momentarily attains its maximum value at $t = t_p$ as the system will pass through the optimum point before it reaches a steady-state. However, since the MPPT algorithm is off, the system could not reach the MPP, and thus, c_p remained far from the c_{pmax} value in steady-state operation as shown in Fig. 11. Then, when the FSA is activated at $t = t_{on}$, the MPP is started to be searched as explained in Sec. III B. The results given in Fig. 11 show how the algorithm progresses toward the MPP.

In Fig. 12, the wind speed has been changed from 8 to 10 m/s in the step-type, while the system is at the MPP. The algorithm has been started to search for a new MPP, and the MPPT has been attained effectively with five steps.

As the third experiment, the wind speed has been changed from 8 to 9 and then 10 m/s as shown in Fig. 13. It is clear from Fig. 13 that the FSA attains the MPPs each wind speed. The performance of the proposed FSA has also been examined for the step-down wind variation as in Fig. 14 and for step-up and step-down wind variations as in Fig. 15.

The results of the experimental studies given above show that the proposed FSA based MPPT algorithm can attain the MPP effectively when the wind speed is changed in step-up and/or step-down form.

V. CONCLUSION

In this paper, a new MPPT method based on the modified FSA has been proposed for the PMSG-based WECS. The general drawbacks of the algorithm-based MPPT methods such as incorrect control

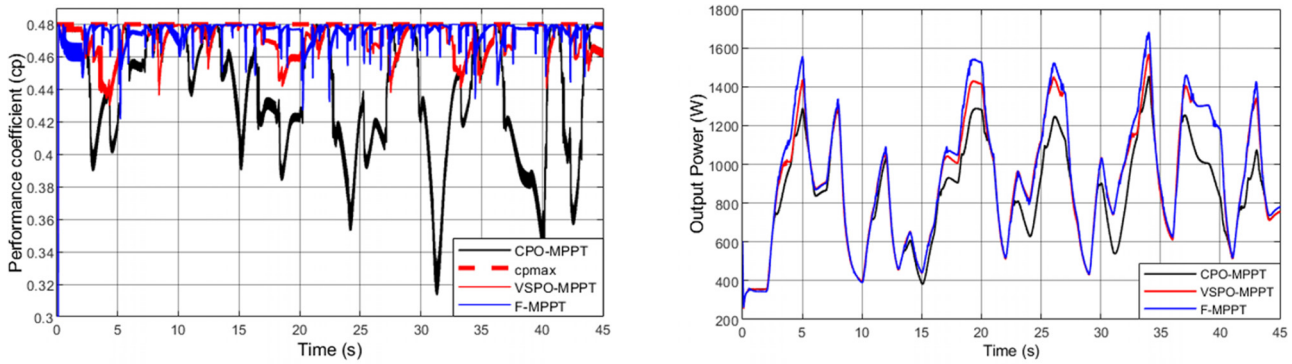

FIG. 9. (a) c_p and (b) P_{out} performances of the methods for Scenario 2.

Published under license by AIP Publishing

TABLE III. The comparison between the methods for Scenario 2.

Performance criteria	CPO	VSPO	Proposed FSA	Available maximum values
Average of c_p	0.4384	0.4710	0.4750	0.48
Average of P_{out} (W)	836.5	924.4	945.5	955.3
Efficiency %	87.56	96.77	98.97	

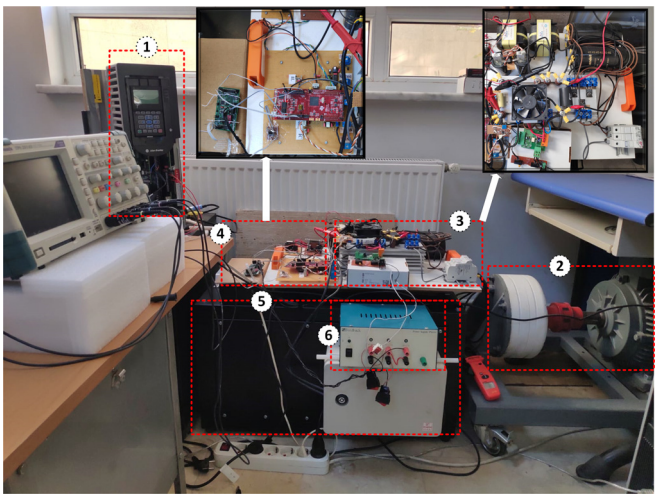

FIG. 10. Picture of the designed test-setup. 1—Induction motor (IM) driver, 2—IM and PMSG, 3—rectifier and boost converter, 4—controller and digital–analog converter (DAC) cards, 5—resistive load, and 6—power supply for the IGBT driver and DAC card.

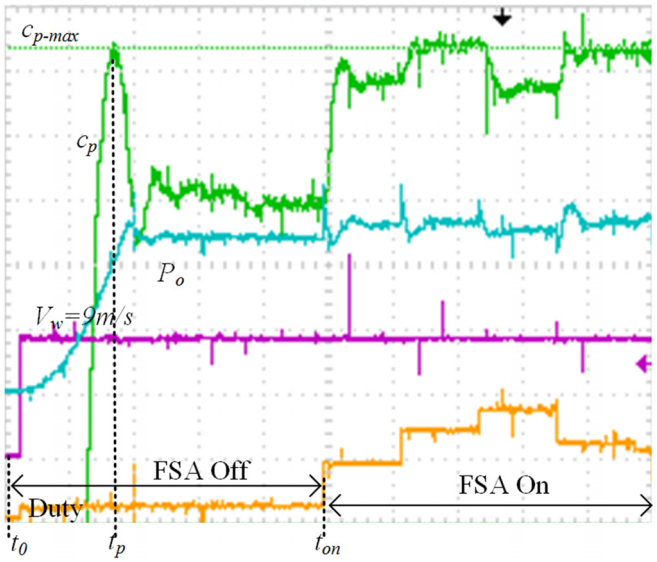

FIG. 11. Experimental results for $V_w = 9$ m/s.

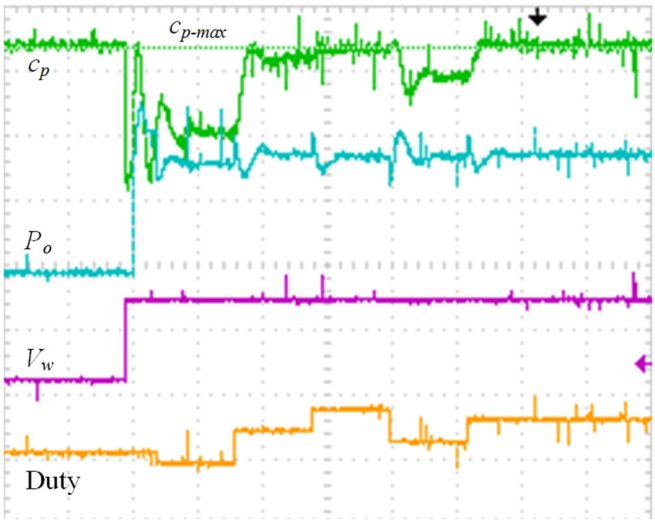

FIG. 12. Experimental results for $V_w = 8$ to 10 m/s.

laws for rapidly changing wind speed, choice of step size, and oscillation around the maximum power are being eliminated via the proposed MPPT algorithm. The performance of the proposed method has been proved with the simulation studies for different wind speeds and stochastic wind speed profiles. Also, the FSA based MPPT method has been compared with the CPO and the VSPO based MPPT methods. The simulation results have approved the superior performance of the proposed method over the CPO and VSPO in terms of the maximum power extracted from the system, namely, efficiency of the WECS. In addition, the real-time experiments carried out for varying wind conditions in the step-up and step-down forms have confirmed that the proposed FSA based algorithm can attain the MPP effectively.

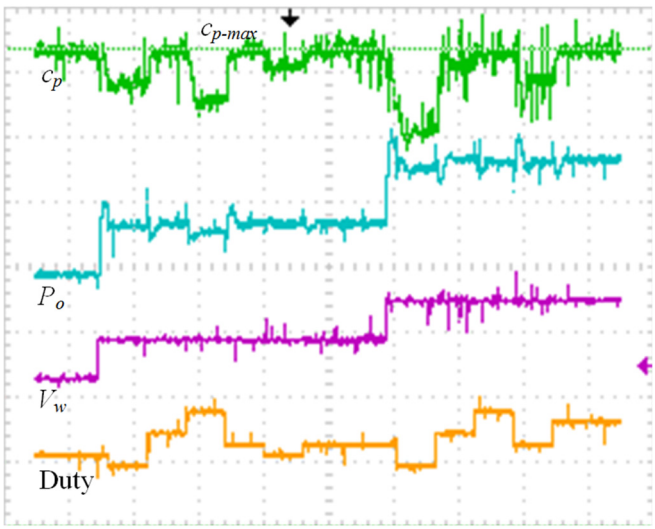

FIG. 13. V_w changed from 8 to 9 and then 10 m/s.

Published under license by AIP Publishing

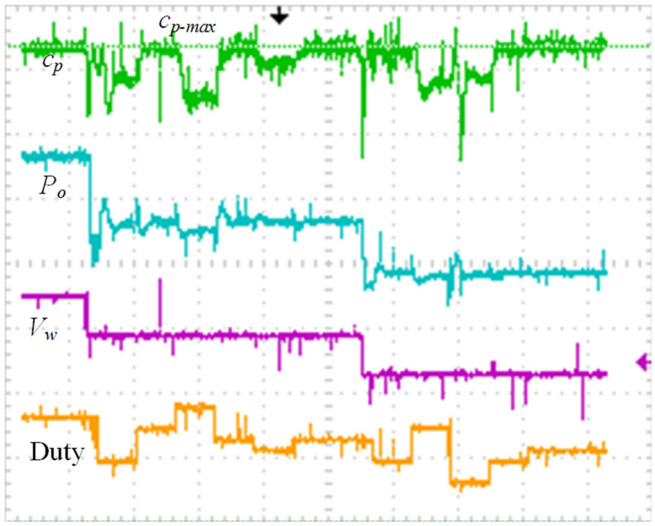

FIG. 14. V_w changed from 10 to 9 and then 8 m/s.

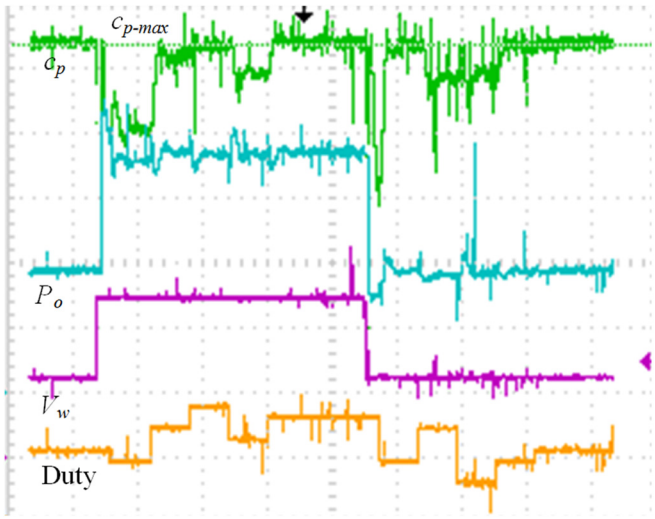

FIG. 15. V_w changed from 8 to 10 and then 8 m/s.

ACKNOWLEDGMENTS

This research was funded by the Scientific and Technological Research Council of Turkey (TÜBİTAK) through a research Grant Account No. 119E284.

DATA AVAILABILITY

The data that support the findings of this study are available from the corresponding author upon reasonable request.

REFERENCES

[1]C. V. Govinda, S. V. Udhay, C. Rani, Y. Wang, and K. Busawon, in Proceedings of the 7th IEEE International Conference on Computation of Power, Energy, Information and Communication (ICCPEIC), 2018, p. 310.
[2]O. Elbeji, M. Hannachi, M. Benhamed, and L. Sbita, Wind Eng. (published online, 2020).
[3]E. H. Dursun and A. A. Kulaksiz, Int. J. Electr. Power Energy Syst. **121**, 106149 (2020).
[4]M. Abolvafaei and S. Ganjefar, Renewable Energy **139**, 1437 (2019).
[5]A. M. Shotorbani, B. Mohammadi-ivatloo, L. Wang, M. Marzband, and M. Sabahi, Electr. Power Energy Syst. **106**, 169 (2019).
[6]I. Yazici and E. K. Yaylaci, J. Energy Res. Technol. **140**, 051203 (2018).
[7]E. K. Yaylacı and I. Yazıcı, J. Renewable Sustainable Energy **10**, 023301 (2018).
[8]R. Errouissi, A. Al-Durra, and M. Debouza, IEEE Trans. Ind. Electron. **65**, 8624 (2018).
[9]K. U. Jadhav and A. G. Thosar, Int. J. Eng. Adv. Technol. **9**, 1321 (2020).
[10]H. H. H. Mousa, A. R. Youssef, and E. E. M. Mohamed, Renewable Energy **145**, 1412 (2020).
[11]E. H. Abdou, A. Youssef, S. Kamel, and M. M. Aly, Int. J. Sci. Eng. Res. **10**, 1682 (2019).
[12]H. H. H. Mousa, A.-R. Youssef, and E. E. M. Mohamed, SN Appl. Sci. **1**, 838 (2019).
[13]H. Ramadan, A.-R. Youssef, H. H. H. Mousa, and E. E. M. Mohamed, SN Appl. Sci. **1**, 1658 (2019).
[14]Soedibyo, A. F. Adila, S. Anam, and M. Ashari, in Proceedings of the International Seminar on Intelligent Technology and its Applications (ISITIA), 2019, p. 114.
[15]R. Kumar, H. P. Agrawal, A. Shah, and H. O. Bansal, Sustainable Energy Technol. Assess. **36**, 100533 (2019).
[16]M. J. Khan and L. Mathew, Int. J. Electron. **105**, 1535 (2018).
[17]F. Ronilaya, B. Setiawan, A. A. Kusuma, I. Mahfudi, and D. M. Yuliawan, IOP Conf. Ser. Mater. Sci. Eng. **407**, 1 (2018).
[18]C. Hung Tran, F. Nollet, N. Essounbouli, and A. Hamzaoui, IOP Conf. Ser. Earth Environ. Sci. **154**, 1 (2018).
[19]K. Parvin, Y. K. Kit, K. P. Jern, M. M. Hoque, and M. A. Hannan, Int. J. Renewable Energy Res. **9**, 164 (2019).
[20]A. A. Salem, N. A. N. Aldin, A. M. Azmy, and W. S. E. Abdellatif, Int. J. Renewable Energy Res. **9**, 1751 (2019).
[21]S. Heshmatian, D. Arab Khaburi, M. Khosravi, and A. Kazemi, Turk. J. Electr. Eng. Comput. Sci. **27**, 2998 (2019).
[22]Y. Zhang, L. Zhang, and Y. Liu, Processes **12**, 1 (2019).
[23]A. Asri, Y. Mihoub, S. Hassaine, P. O. Logerais, and T. Allaoui, Asian J. Control **21**, 1980 (2019).
[24]M. Mekki, T. Allaoui, B. Belabbas, and M. Denai, Przegląd Elektrotech. **1**, 114 (2020).
[25]E. H. Dursun, H. Koyuncu, and A. A. Kulaksiz, Eng. Sci. Technol. Int. J. **24**, 158–170 (2021).
[26]I. Yazici and E. K. Yaylaci, J. Energy Resour. Technol. Trans. ASME **140**, 1 (2018).
[27]E. K. Yaylacl and I. Yazlcl, J. Renewable Sustainable Energy **10**, 023301 (2018).
[28]S. Sabzevari, A. Karimpour, M. Monfared, M. Bagher, N. Sistani, S. Sabzevari, A. Karimpour, M. Monfared, and M. B. Naghibi Sistani, J. Renewable Sustainable Energy **9**, 013302 (2017).
[29]A. Sachan, A. K. Gupta, and P. Samuel, J. Green Eng. **6**, 385 (2017).
[30]L. Liu, X. Meng, and C. Liu, Renewable Sustainable Energy Rev. **53**, 1500 (2016).
[31]J. H. Zhang, X. Y. Wei, L. Hu, and J. G. Ma, Teh. Vjesn. **26**, 163 (2019).
[32]M. N. Masafumi Miyatake and T. Kouno, in Proceedings of the International Conference on Pharmacoepidemiology (ICPE), Seoul, 2001, pp. 622–625.
[33]M. Miyatake, T. Inada, I. Hiratsuka, H. Zhao, H. Otsuka, and M. Nakano, in Proceedings of the 4th International Power Electronics and Motion Control Conference (IPEMC), Riga, Latvia, 2004, pp. 816–821.
[34]N. A. Ahmed and M. Miyatake, Electr. Power Syst. Res. **78**, 777 (2008).
[35]R. Ramaprabha, B. Mathur, A. Ravi, and S. Aventhika, in *Proceedings of the International Conference of Emerging Trends in Engineering and Technology* (IEEE, Goa, India, 2010), pp. 379–384.

Published under license by AIP Publishing

[36]R. Ramaprabha, M. Balaji, and B. L. Mathur, Int. J. Electr. Power Energy Syst. **43**, 754 (2012).
[37]S. Malathy and R. Ramaprabha, in *Proceedings of the International Conference on Power Electronics and Drive Systems* (IEEE, Honolulu, HI, 2017), pp. 487–492.
[38]C. Zhao-Zhang, Z. Xin-Liang, and W. Quin-Wei, Power Electron. **53** (2008), see https://en.cnki.com.cn/Article_en/CJFDTOTAL-DLDZ200805023.htm.
[39]B. Amlang, D. Arsurdis, W. Leonhard, W. Vollstedt, and K. Wefelmeier, *Elektrische Energieversorgung Mit Windkraftanlagen* (Abschlußbericht BMFT-Forschungsvorhaben 032-8265-B, Braunschweig, 1992).
[40]H. S. Kim and D. D.-C. Lu, in Proceedings of the Australasian Universities Power Engineering Conference, New Zealand, 2010, pp. 1–6.
[41]A. M. Eltamaly and H. M. Farh, Electr. Power Syst. Res. **97**, 144 (2013).
[42]K. Tan and S. Islam, IEEE Trans. Energy Convers. **19**, 392 (2004).
[43]R. Esmaili, L. Xu, and D. K. Nichols, in Proceedings of the IEEE Power Engineering Society General Meeting, San Francisco, CA, 2005, pp. 1–6.
[44]M. A. Abdullah, A. H. M. Yatim, C. W. Tan, and R. Saidur, Renewable Sustainable Energy Rev. **16**, 3220 (2012).
[45]H. Fathabadi, Optim. Control Appl. Methods **39**, 1354 (2018).
[46]H. Fathabadi, IEEE J. Emerging Sel. Top. Power Electron. **5**, 1739 (2017).
[47]G. Technologies, see www.milenerji.com.tr/wp-content/uploads/Ginlong_Catalogue.pdf.
[48]D. W. Hart, *Power Electronics* (McGraw-Hill, Valparaiso, Indiana, 2011).
[49]H. H. H. Mousa, A. R. Youssef, and E. E. M. Mohamed, Int. J. Electr. Power Energy Syst. **112**, 294 (2019).
[50]M. M. Ali, A. R. Youssef, A. S. Ali, and G. T. Abdel-Jaber, Int. Trans. Electr. Energy Syst. **30**, e12151 (2019).
[51]S. S. Rao, *Engineering Optimization: Theory and Practice*, 4th ed. (John Wiley and Sons, Inc., 2009).
[52]I. Yazıcı and E. K. Yaylacı, IET Power Electron. **12**, 3688 (2019).
[53]E. K. Yaylacı and I. Yazıcı, Gazi Univ. Fen Bilim. Derg. Part C Tasarım Teknol. **7**, 175 (2019).

Published under license by AIP Publishing